

## Supporting Information

### **Synthesis, characterization and insights into stable and well organized hexagonal mesoporous zinc-doped alumina as promising metathesis catalysts carrier**

Abdelnasser Abidli,<sup>a,b</sup> Safia Hamoudi<sup>a,b</sup> and Khaled Belkacemi\*<sup>a,b</sup>

<sup>a</sup> *Department of Soil Sciences and Agri-Food Engineering, Laval, University. G1V 0A6, Quebec City, Quebec, Canada. E-mail: khaled.belkacemi@fsaa.ulaval.ca; Fax: +1-418-656-3723; Tel: +1-418-656-2131 ext: 6511*

<sup>b</sup> *Centre in Green Chemistry and Catalysis (CGCC), H3A 0B8, Montreal, Quebec, Canada*

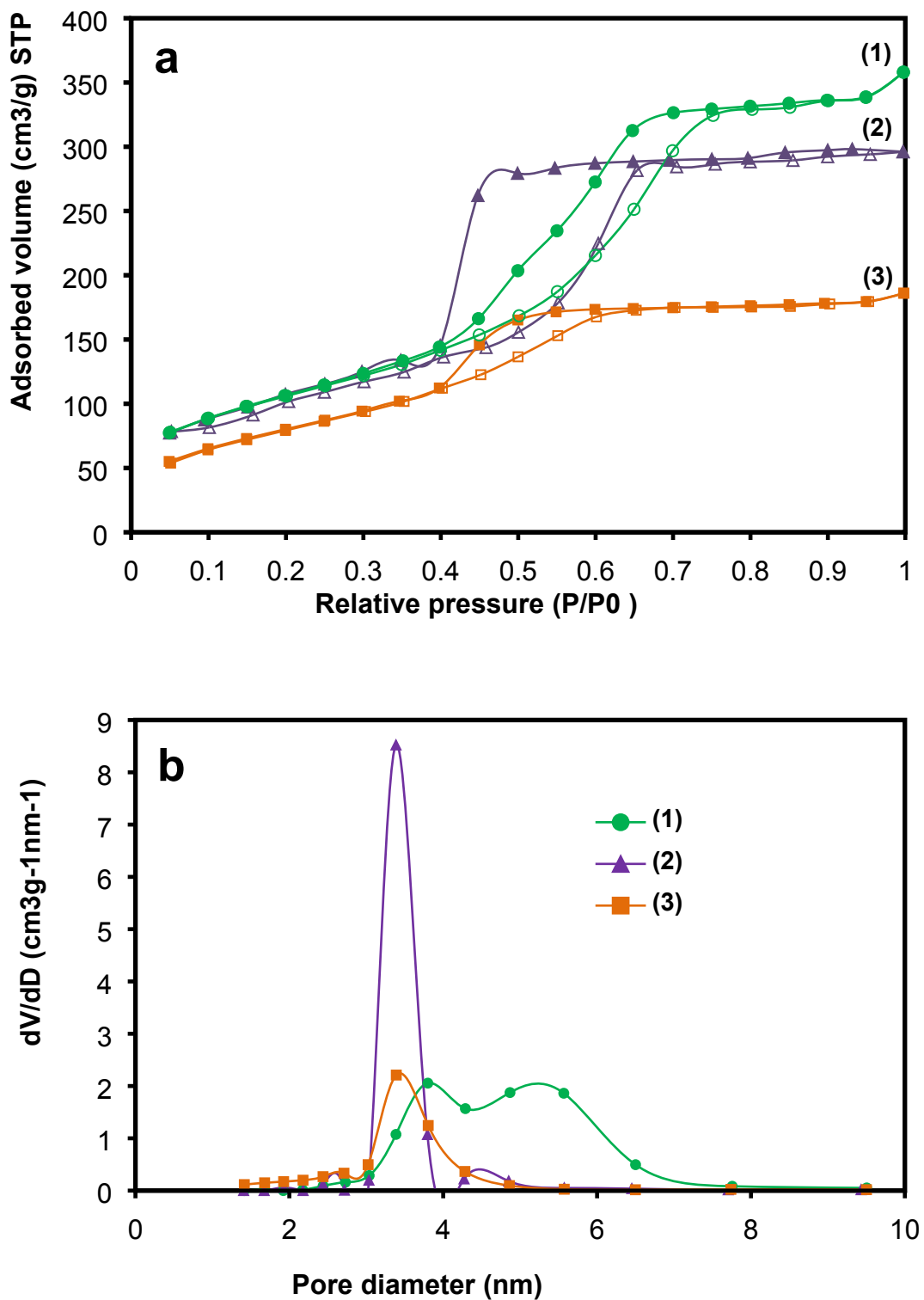


**Figure S1.** (a) Nitrogen adsorption–desorption isotherms and (b) BJH pore size distributions curves of the prepared OMA samples: (1) Al<sub>2</sub>O<sub>3</sub>-acetic, (2) Al<sub>2</sub>O<sub>3</sub>-citric, (3) Al<sub>2</sub>O<sub>3</sub>-malonic.

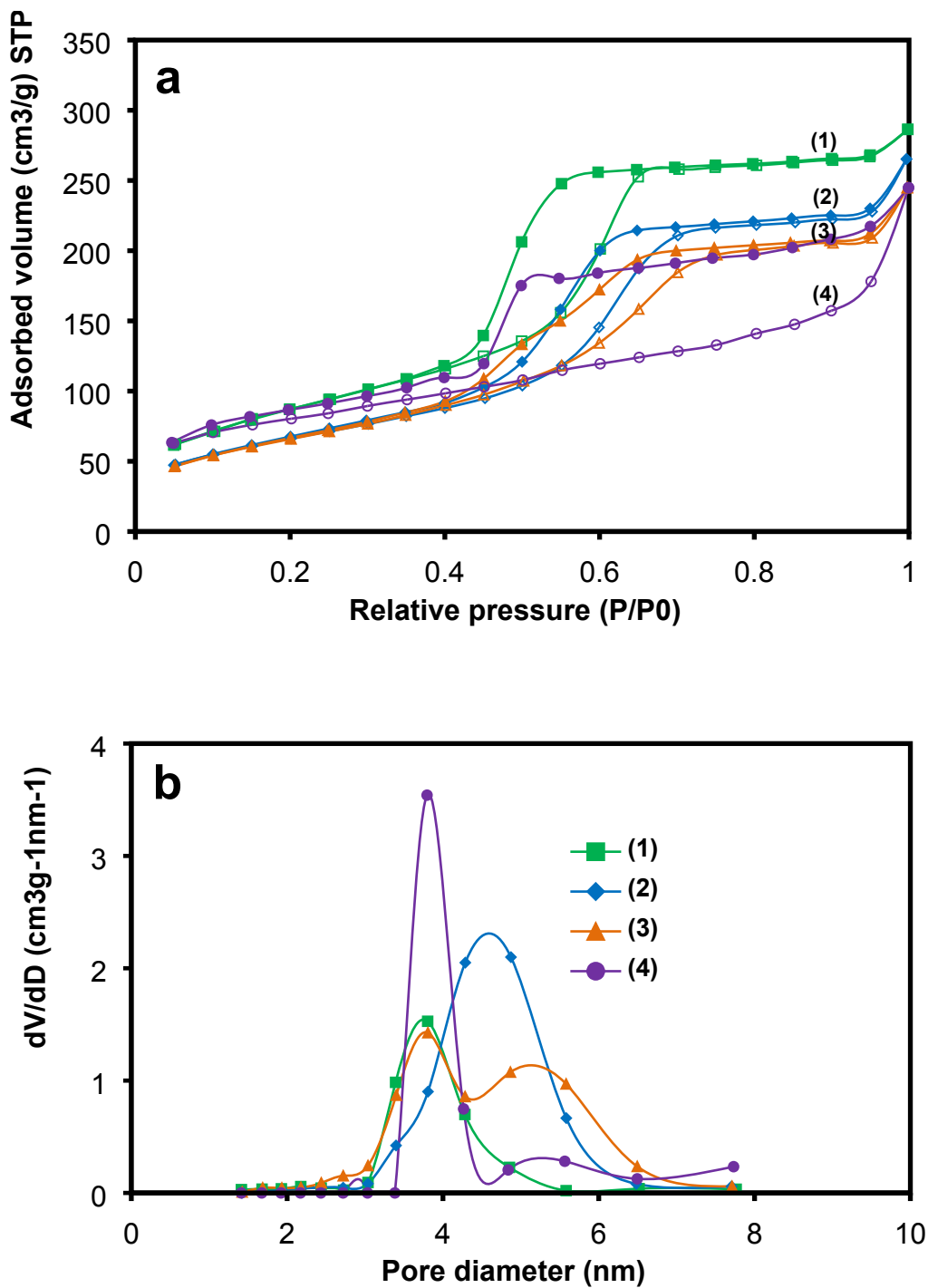


**Figure S2.** (a) Nitrogen adsorption–desorption isotherms and (b) BJH pore size distributions curves of the prepared zinc chloride modified-OMA samples using citric acid with different aluminum precursors: (1)  $\text{ZnCl}_2\text{-Al}_2\text{O}_3\text{-Al}(\text{O}i\text{Bu})_3$ , (2)  $\text{ZnCl}_2\text{-Al}_2\text{O}_3\text{-Al}(\text{O}n\text{Bu})_3$ , (3)  $\text{ZnCl}_2\text{-Al}_2\text{O}_3\text{-Al}(\text{OPr}^i)_3$  and (4)  $\text{ZnCl}_2\text{-Al}_2\text{O}_3\text{-Al}(\text{NO}_3)_3 \cdot 9\text{H}_2\text{O}$ . All samples were calcined at 400 °C.

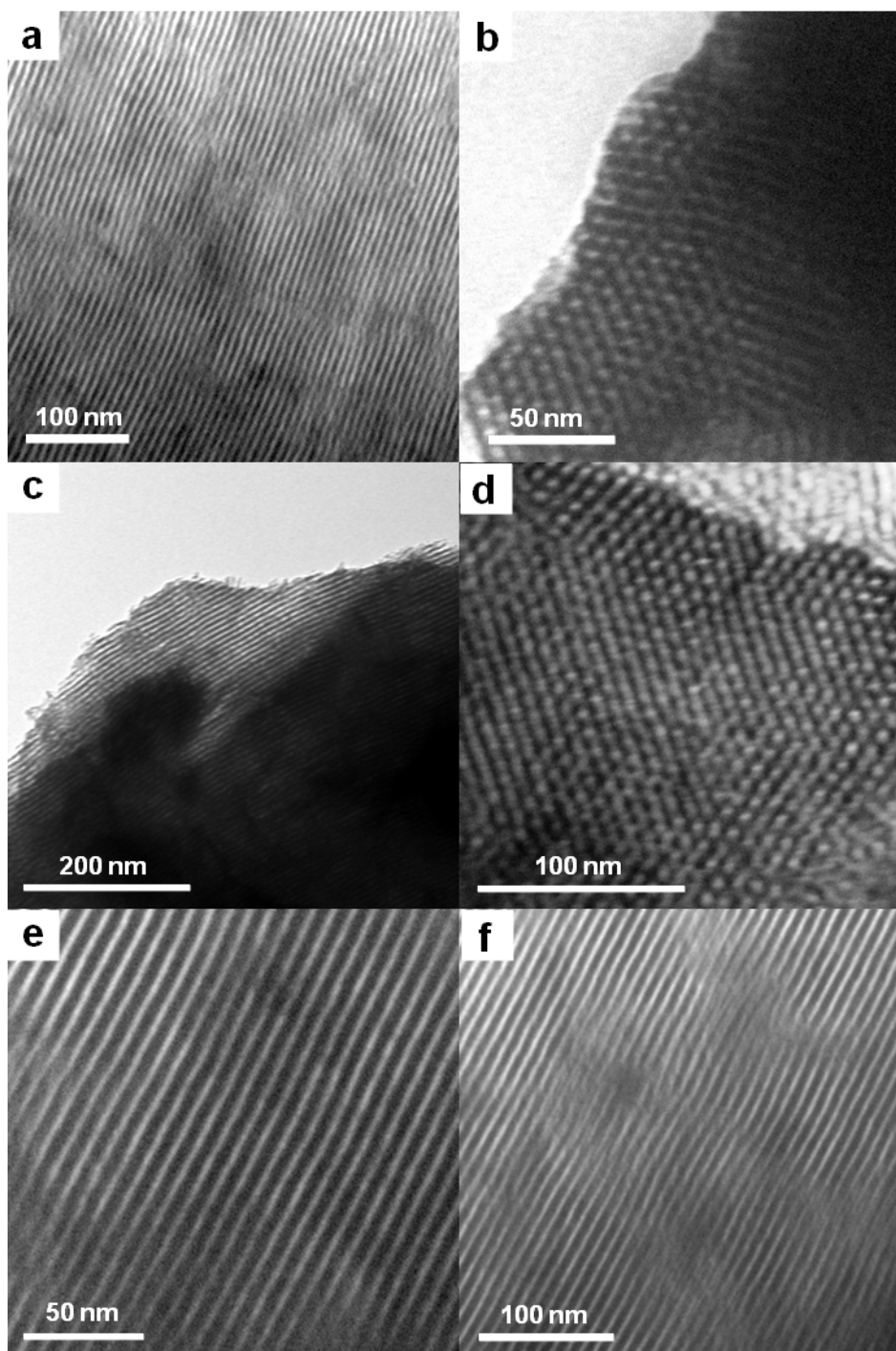


**Figure S3.** TEM micrographs of the prepared zinc chloride-modified ordered mesoporous alumina materials with different carboxylic acids; (a) citric, (c) oxalic, (e) tartaric and (f) fumaric viewed along [001] orientation and (b) maleic and (d) malonic viewed along [110] orientation.

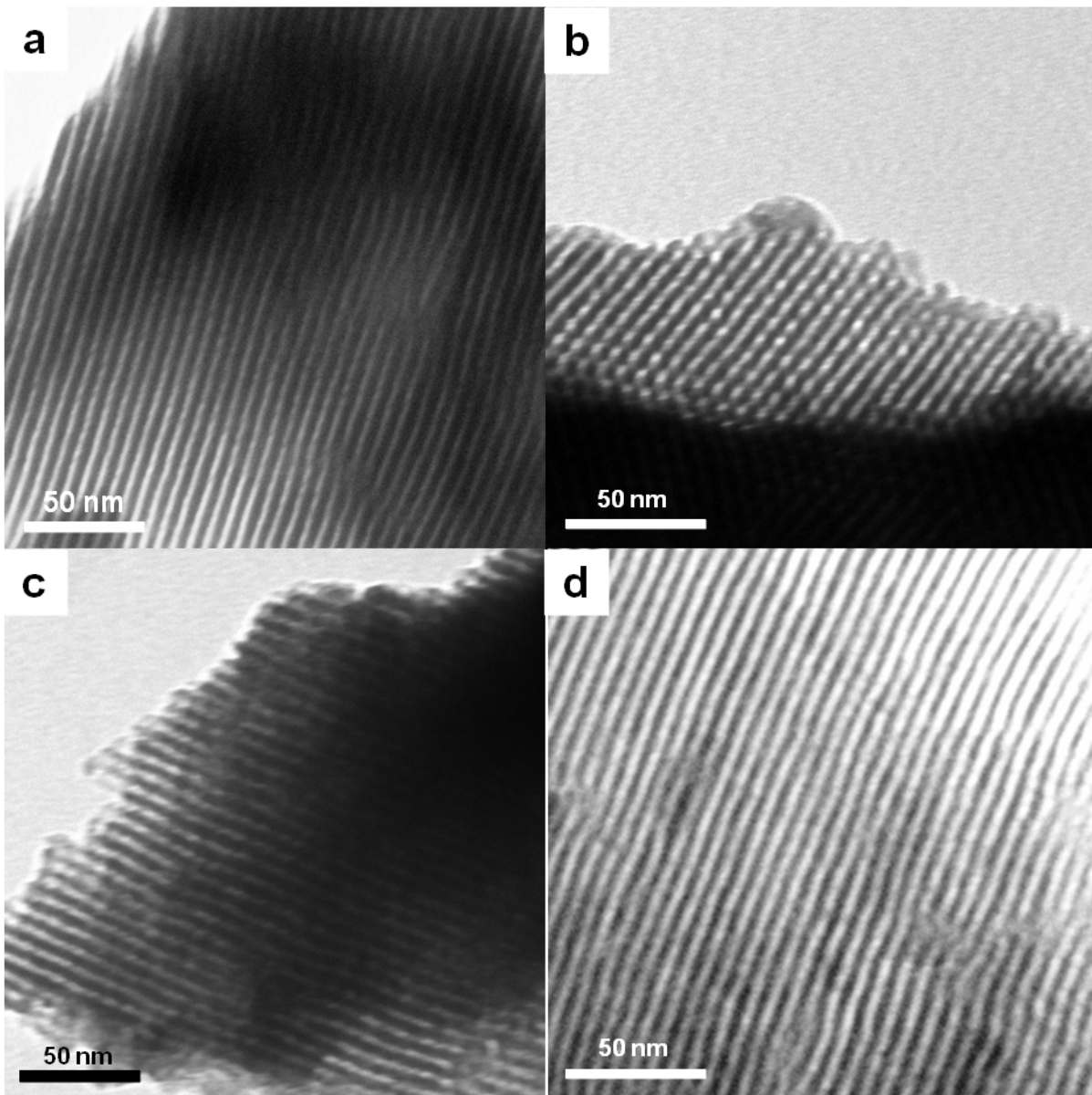


**Figure S4.** TEM micrographs of the prepared zinc chloride-modified OMA using tartaric acid with different aluminum precursors; with (a) aluminum isopropoxide, (c) aluminum nitrate nonahydrate and (d) aluminum-tri-*sec*-butoxide viewed along [001] orientation, and (b) aluminum tri-*tert*-butoxide viewed along [110] orientation.

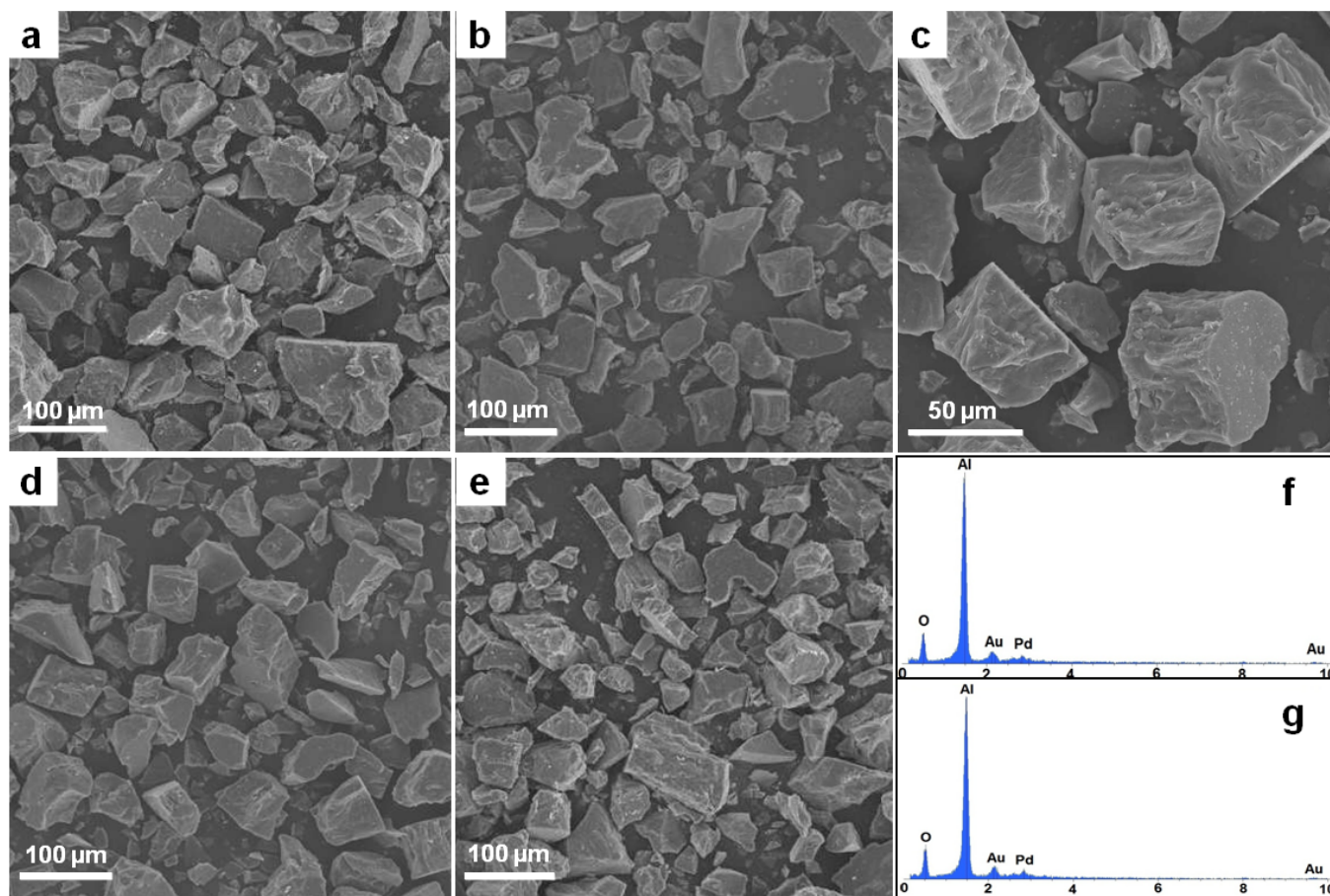


**Figure S5.** Representative SEM images obtained for OMA microparticles prepared using  $\text{Al}(\text{OBU}^s)_3$  with different carboxylic acids: (a) fumaric, (b) tartaric (c, d) oxalic and (e) citric. Energy dispersive X-ray (EDX) spectra of OMA samples obtained using (f) oxalic and (g) fumaric acid.

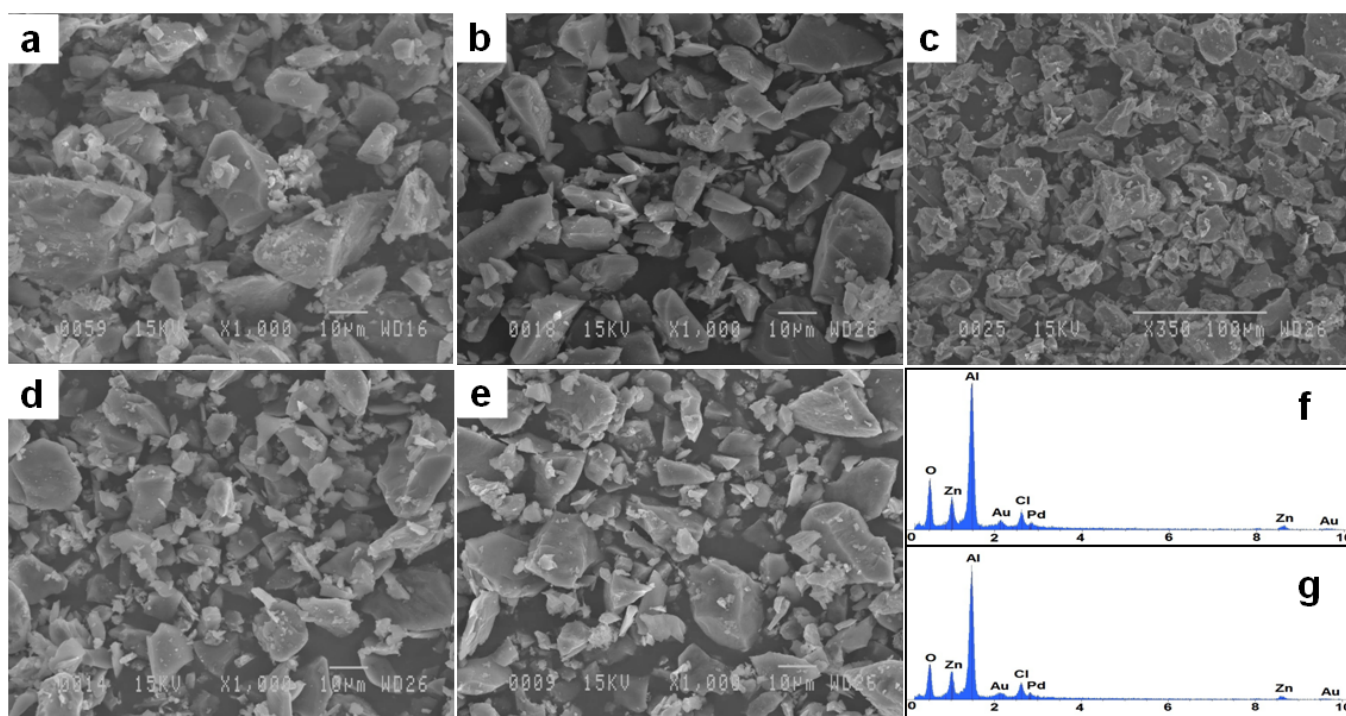


**Figure S6.** Representative SEM images obtained for zinc chloride-modified OMA microparticles prepared using different carboxylic acids and aluminum precursors: (a) tartaric-Al(OPr<sup>t</sup>)<sub>3</sub>, (b) tartaric-Al(OBu<sup>t</sup>)<sub>3</sub>, (c) citric-Al(OBu<sup>s</sup>)<sub>3</sub>, (d) oxalic-Al(OBu<sup>s</sup>)<sub>3</sub> and (e) oxalic-Al(NO<sub>3</sub>)<sub>3</sub> · 9H<sub>2</sub>O. Energy dispersive X-ray (EDX) spectra of ZnCl<sub>2</sub>-OMA samples obtained using Al(OBu<sup>s</sup>)<sub>3</sub> with (f) fumaric and (g) citric acid.

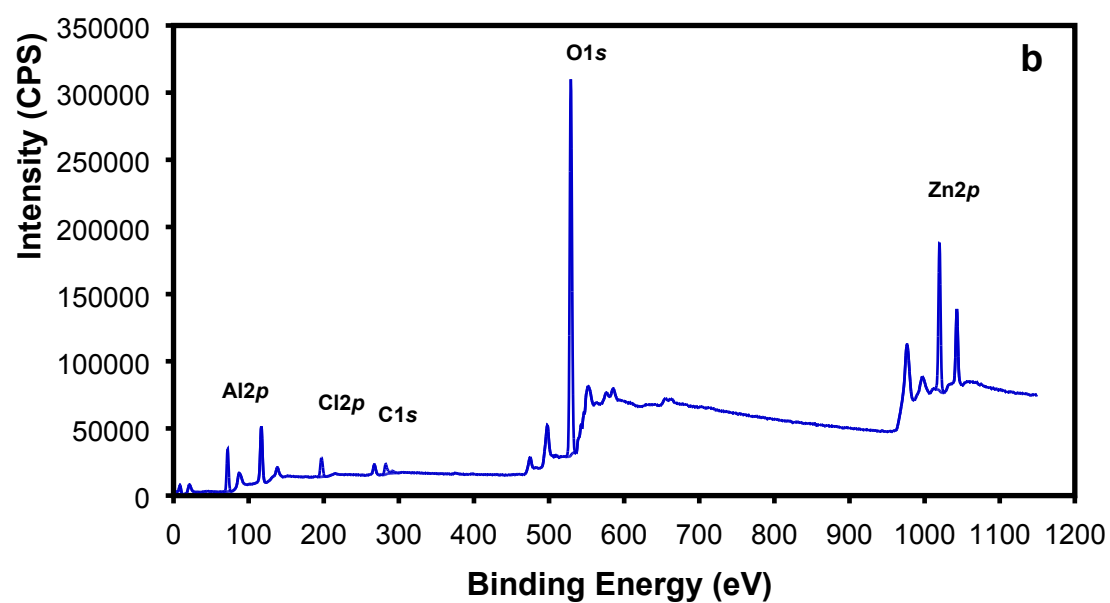
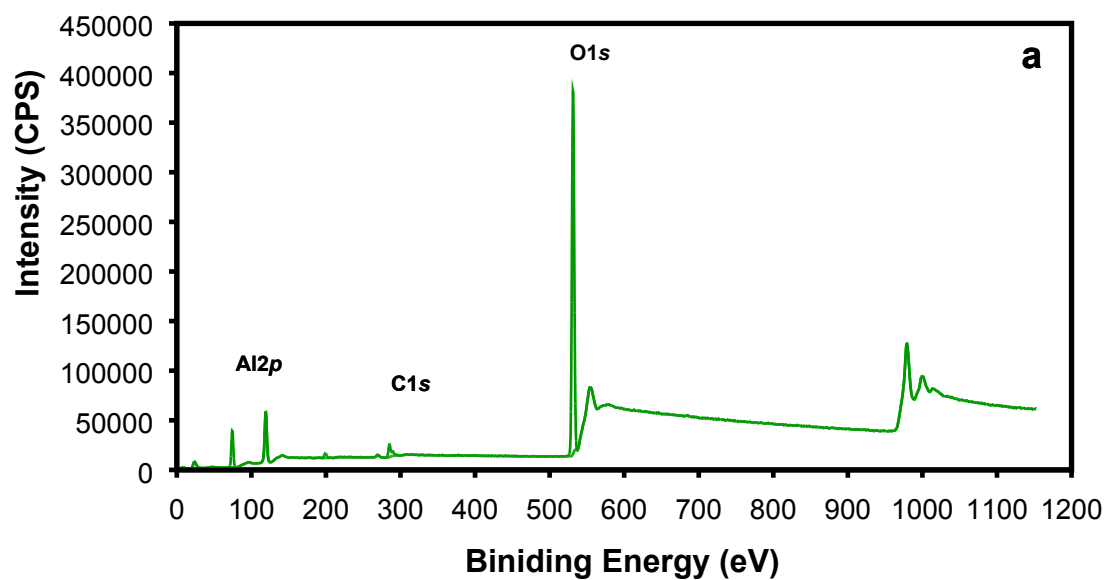


**Figure S7.** XPS survey spectra of (a) the OMA and (b) the ZnCl<sub>2</sub>-modified OMA samples.